Novel Sequential Error-Concealment Techniques Using Orientation Adaptive Interpolation

Xin Li, *Member, IEEE*, and Michael T. Orchard, *Fellow, IEEE*

***Abstract*—This paper introduces a new framework for error concealment in block-based image coding systems: sequential recovery. Unlike previous approaches that simultaneously recover the pixels inside a missing block, we propose to recover them in a sequential fashion such that the previously-recovered pixels can be used in the recovery process afterwards. The principal advantage of the sequential approach is the improved capability of recovering important image features brought by the reduction in the complexity of statistical modeling, i.e., from blockwise to pixelwise. Under the framework of sequential recovery, we present an orientation adaptive interpolation scheme derived from the pixelwise statistical model. We also investigate the problem of error propagation with sequential recovery and propose a linear merge strategy to alleviate it. Extensive experiment results are used to demonstrate the improvement of the proposed sequential error-concealment technique over previous techniques in the literature.**

***Index Terms*—Error concealment, error propagation, linear merge, orientation adaptive interpolation, sequential recovery.**

I. Introduction

BLOCK-BASED image coding systems have been extensively studied for efficient transmission of visual signals. Most existing image and video compression standards such as JPEG [1] and MPEG [2] structure an image into nonoverlapped blocks and process them separately. When the encoded bit stream goes through a time-varying channel such as wireless or ATM network, it is vulnerable to the channel impairment. In the block-based image coding system, the loss of one single bit often results in the loss of the whole block, which seriously affects the visual quality of decoded images at the receiver. The error-concealment technique is an attractive approach that takes advantage of the spatial correlation within images to alleviate the negative effect of information loss. It can be viewed as a post-processing stage to fight against the channel impairment without incurring any overhead or delay.

In practice, both the source quantization and the channel impairment introduce distortion to the decoded image at the receiver. However, the distortion brought by the source quantization depends on the specific quantization algorithm, which is often difficult to model [19]. A simplified formulation of the error-concealment problem is to only consider the effect of channel impairment. That is, all successfully received blocks are treated identical to the original blocks. In the meantime, we shall assume that the locations of corrupted blocks are known before error concealment is employed at the receiver. Such information can be obtained either at the transport decoder or at the source decoder [18].

The performance of any error-concealment technique depends on the accuracy of the model used to characterize the image source in a variety of block-loss situations. Most existing error-concealment techniques [3]–[14] employ blockwise deterministic models in either the spatial or the spectral domain to describe the spatial dependency within images. References [3], [6] estimate the lost discrete cosine transform (DCT) coefficients in the spectral domain based on the spatial smoothing constraint on the reconstructed blocks. Simplified edge models are imposed in [5], [7], [9], and [14] to derive directional interpolation in the spatial domain. Other approaches include fuzzy logic reasoning [8], best neighbor matching [10], maximally smooth recovery [12], and projection-onto-convex-set (POCS) [4], [13]. All those techniques simultaneously recover the pixels inside the missing block, which we call *parallel recovery*.

In this paper, we present a new framework for error-concealment techniques: *sequential recovery*. The image data in the corrupted block are recovered in a sequential fashion such that the recovery relies on not only successfully received pixels, but also previously recovered ones. From a statistical point of view, sequential recovery can be viewed as transforming the original MAP estimation problem that requires a blockwise conditional probabilistic model into a series of easier MAP estimation problems that only require a pixelwise conditional probabilistic model. Such transformation substantially alleviates the complexity of statistical modeling (i.e., from blockwise to pixelwise) and offers a ground for the development of new error-concealment techniques. The principal advantage of sequential recovery over parallel recovery is the improved capability of modeling important image features such as edges. Previous parallel approaches attempt to explicitly resolve the uncertainty of edge orientation and edge quantity based on geometric analysis. However, the reliability of geometric analysis often becomes questionable when there are more than one edge inside the corrupted block and when not all the neighboring blocks are successfully received. Consequently, the reconstructed images by parallel recovery might suffer from edge blurring or various artifacts (e.g., false edge). In contrast, sequential recovery based on pixelwise statistical models enjoys more flexibility of inferring important edge features from local available information.

It should be noted that the Markov random field (MRF)-based approach in [15] can also be viewed as pixelwise statistical modeling because MRF allows modeling a priori information from a small local neighborhood. However, the MRF-based

Manuscript received November 17, 2000; revised January 15, 2002. This paper was recommended by Associate Editor R. L. Stevenson.

X. Li is with Sharp Laboratories of America, Camas, WA 98607 USA (e-mail: xli@sharplabs.com).

M. T. Orchard is with the Department of Electrical and Computer Engineering, Rice University, Houston, TX 77005 USA (e-mail: orchard@ece.rice.edu).

Digital Object Identifier 10.1109/TCSVT.2002.804882

model has its fundamental limitation of characterizing nonstationarity in the image. Within the framework of sequential recovery, we present a novel orientation adaptive interpolation scheme in Section III. Under the assumption that a nonstationary image can still be locally modeled as a stationary Gaussian process, we estimate the covariance characteristics inside a local window and use them to locally adapt the interpolation coefficients. Such covariance-based adaptation method is capable of tuning the support of the interpolation to match an arbitrarily oriented edge and has demonstrated impressive performance in lossless image compression [16].

Despite the above advantage, sequential recovery suffers from the error-propagation problem because previously recovered pixels are also used to resolve the uncertainty of missing pixels in addition to the successfully received pixels. Due to the introduced sequential recovery structure, different scanning orders would result in different error-propagation patterns and affect the recovery performance. Recognizing the difficulty of finding the universally optimal scanning order in various block-loss situations, we choose to take an approach of linear merge in Section IV to fight against error propagation. Though the scanning order is fixed (we choose the conventional raster scanning for its simplicity), we propose to recover the corrupted block from eight different scanning orientations and take their linear merge as the final result. Substantial improvement on the performance has been achieved by the linear merge strategy at the price of increased computational complexity by a factor of eight.

It is interesting to point out the linkage of our work to the well-known iterated conditional modes (ICM) method [17]. Both our approach and ICM attempt to maximize the conditional probability of each individual pixel given the observations and the other pixel estimates. However, ICM employs the Bayes' rule on the posterior probability to yield an optimization with the prior probability and the likelihood. For images, prior probability model is often not available or not accurate enough. Our work is based on the assumption that the image can be locally modeled as a stationary Gaussian process, and thus statistical modeling complexity reduces to the estimation of local covariance characteristics only. Another major difference between our work and ICM is that we employ a noniterative linear merge strategy. Theoretically, it is also possible to perform our scheme in an iterative fashion; but the computational complexity will become prohibitive. The proposed linear merge strategy can be viewed as a low complexity approximation of the solution to a global stochastic optimization problem.

The rest of this paper is organized as follows. Section II starts from the formulation of the error-concealment problem and discusses both parallel and sequential recovery from statistical point of view. Section III presents the new orientation adaptive interpolation in the framework of sequential recovery. Section IV studies the error propagation and introduces the linear merge strategy. Extensive experiment results are included in Section V. Finally, we make our concluding remarks about this work in Section VI.

II. Problem Formulation

The error-concealment problem deals with the estimation of some corrupted blocks from their neighboring blocks that have been successfully received at the decoder. According to the availability of the neighboring blocks, we can classify the block-loss situations into two types: *isolated* block loss and *consecutive* block loss. If the eight surrounding blocks of the missing block are all successfully received, we treat it as isolated block loss; otherwise, it is consecutive block loss. Fig. 1 shows the examples in different block-loss situations.

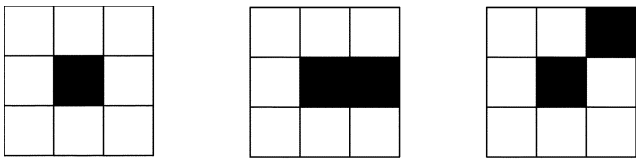

Fig. 1. (a) Isolated block loss. (b) Consecutive block loss (horizontal). (c) Consecutive block loss (diagonal).

From a statistical point of view, the error-concealment problem can be viewed as the recovery of one subset of pixels X_k $(1 \le k \le K)$ from the other subset of pixels Y_l $(1 \le l \le L)$ within the image. The MAP estimation of X_k can be written as

$$X_1, \ldots, X_K \text{ s.t. maximize } p(X_1, \ldots, X_K | Y_1, \ldots, Y_L).$$

However, it is almost impossible to obtain the above conditional probability distribution in practice because the dimensionality K (block size) is too large. One way to simplify the above problem is to recover each X_k in the following parallel fashion:

$$\text{for every } k = 1, \ldots, K, \quad \text{maximize } p(X_k | Y_1, \ldots, Y_L).$$

In fact, $p(X_1, \ldots, X_K | Y_1, \ldots, Y_L)$ differs from $\prod_{k=1}^{K} p(X_k | Y_1, \ldots, Y_L)$ due to the spatial correlation among the X_k's. Therefore, blockwise prior models are often employed to characterize the dependency within the missing blocks. For example, simplified edge models controlled by the quantity and the orientation of edges [9], [8], [14] are often used to adapt the local interpolation. The smoothness constraint and the edge continuity in the spectral or the spatial domain [4], [3], [12] are also popular models to emphasize the integrity of local edge structures. Unfortunately, the accuracy and the robustness of those models are often limited by their blockwise structures.

Another popular approach to the MAP estimation problem is to use Bayes' rule [21]. It transforms the posterior probability to the prior probability term and the likelihood term. In some sense, such an approach can be also viewed as parallel recovery. The major limitation with Bayes' formulation is that the prior probability model for the image source is not directly available or not accurate enough. For example, MRF [15] is one of widely used models for images; but its capability of characterizing nonstationary features (edges) in an image is limited. Consequently, the subjective quality of recovered images using MRF model is often unsatisfactory around edges.

In this paper, we present a new framework for solving the above MAP estimation problem, that is, to transform it into the following equivalent problem:

$$\text{for every } k = 1, \ldots, K, \quad \text{maximize } p(X_k | X_1, \ldots, X_{k-1}, Y_1, \ldots, Y_L)$$

and we note that

$$p(X_1, \ldots, X_K|Y_1, \ldots, Y_L) = \prod_{k=1}^{K} p(X_k|X_1, \ldots, X_{k-1}, Y_1, \ldots, Y_L). \quad (1)$$

From (1), we can see that the original blockwise conditional probability distribution function is decomposed into a series of pixelwise conditional probability distribution functions. Such decomposition provides ground for developing more accurate and more robust error-concealment techniques.

The principal advantage from the above sequential structure is the improved capability of recovering important image features such as edges, especially in the following two scenarios: 1) when there are more than one edge inside the missing block and 2) when the block loss is consecutive. In those scenarios, parallel approaches using blockwise prior models often can not reliably estimate the quantity and the orientation of the edge features. Consequently, reconstructed images would suffer from either blurred edges or annoying artifacts. In contrast, since sequential recovery employs pixelwise models to characterize the dependency within images, it offers the flexibility of using local available information to adapt the recovery process such that important edge features are well preserved in the reconstructed images.

Within the framework of sequential recovery, the first problem we want to address is how to solve the individual MAP estimation problem, i.e., maximize $p(X_k|X_1, \ldots, X_{k-1}, Y_1, \ldots, Y_L)$. Motivated by our recent work on lossless image compression [16], we present a novel orientation-adaptive interpolation scheme in Section III. We estimate the local covariance characteristics from both $X_1, \ldots, X_{k-1}$ and $Y_1, \ldots, Y_L$ and use them to derive an optimal interpolation for the missing pixel. Since we do not have the access to the original $X_1, \ldots, X_{k-1}$ but only their recovered values in practice, error propagation is inevitable, and the choice of scanning order plays the critical role on the recovery performance. Therefore, the second problem under investigation is how to alleviate the error propagation associated with a specific scanning order. Recognizing the difficulty with finding a universally optimal solution to various block-loss situations, we propose to fix the scanning order (i.e., we only consider raster scanning for its simplicity in this paper), but change the scanning orientation. A natural but effective strategy of fighting against error propagation is to linear weight the reconstructed images from different scanning orientations. We will discuss the design of weighting coefficients in our linear merge strategy in Section IV.

III. Orientation-Adaptive Interpolation

This section addresses the problem of interpolating a corrupted pixel X_n from its available neighbors. The available neighbors could be either successfully received pixels $Y_l (l = 1, \ldots, L)$ or previously recovered pixels $X_k (k = 1, \ldots, n-1)$. To facilitate the description, we will use the set $M_n = \{X_{n-1}, X_{n-2}, \ldots, X_1, X_0 = Y_1, \ldots, X_{n-M} = Y_L\}, M = n + L - 1$ to denote all available neighbors of X_n no matter it is successfully received or previously recovered (i.e., we do not distinguish Y_l and X_k any more). The atomic problem in sequential recovery is to obtain the optimal estimation of X_n in the sense of maximizing $p(X_n|M_n)$.

We make the following assumptions that reasonably hold for an image source.

1) Although globally the image source can not be modeled by a stationary Gaussian process, it can be viewed as locally stationary. Therefore, the conditional probability distribution function $p(X_n|M_n)$ is mostly characterized by the second-order statistics (covariance).
2) The image source satisfies the Nth-order Markov property, i.e., $p(X_n|X_{n-1}, X_{n-2}, \ldots) = p(X_n|X_{n-1}, \ldots, X_{n-N})$.

Under those assumptions, it can be shown that the MAP estimation problem boils down to the linear minimum mean-square error (MMSE) estimation problem of minimizing $E\{(X_n - \hat{X}_n)^2\}$, where $\hat{X}_n$ is the linear estimation of X_n based on $N_n = \{X_{n-1}, \ldots, X_{n-N}\}$

$$X_n = \sum_{k=1}^{N} a_k X_{n-k}. \quad (2)$$

According to the classical Wiener filtering theory [20], the optimal coefficients $\vec{a} = [a_1 \cdots a_N]^T$ are only determined by the second-order statistics (covariance) of the Gaussian process

$$\vec{a} = (R_{XX})^{-1}\vec{r}_X \quad (3)$$

where $\vec{r}_X = [r_1 \cdots r_k \cdots r_N], r_k = Cov\{X_n X_{n-k}\}$ $(1 \le k \le N)$ and $R_{XX} = [R_{kl}], R_{kl} = Cov\{X_{n-k}X_{n-l}\}$ $(1 \le k, l \le N)$. Geometrically, (3) is the projection of X_n onto the subspace spanned by $X_{n-1} \cdots X_{n-N}$ in the least-square sense. Due to the assumption of a locally stationary process, the covariance can be estimated inside a local window using a conventional "covariance method" [20]

$$\hat{R}_{XX} = C^T C, \quad \hat{\vec{r}}_X = C^T \vec{y} \quad (4)$$

where $\vec{y} = [X_{n-1} \cdots X_{n-M}]^T$ is an $M \times 1$ vector containing all the elements inside the local window M_n and

$$C = \begin{bmatrix} X_{n-1-1} & \cdots & X_{n-1-N} \\ \vdots & & \vdots \\ X_{n-M-1} & \cdots & X_{n-M-N} \end{bmatrix}$$

is an $M \times N$ matrix whose kth row consists of the N neighbors used to estimate X_{n-k}. By plugging (4) into (3), we obtain

$$\vec{a} = (C^T C)^{-1}(C^T \vec{y}). \quad (5)$$

The above approach of estimating X_n can be viewed as covariance-based adaptive interpolation. It has been justified in [16] that such covariance-based adaptation is capable of tuning the support of $\vec{a}$ to get aligned along an arbitrary edge orientation. Therefore, (5) often better preserves the important edge features than naive linear interpolation techniques that assign the fixed interpolation coefficients uniformly for the whole image.

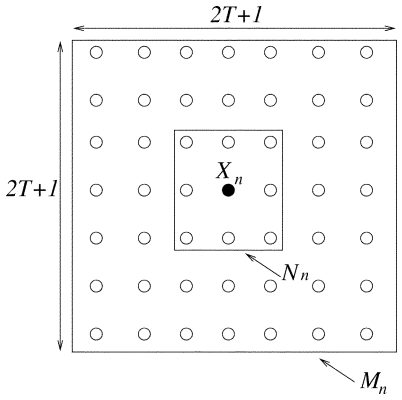

Fig. 2. Definition of M_n and N_n.

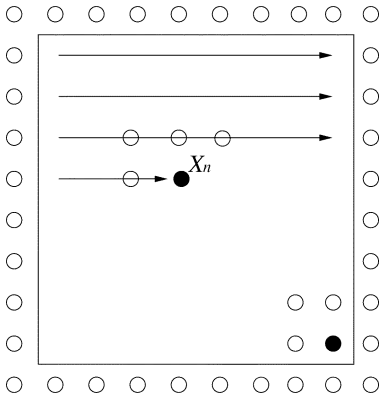

Fig. 3. Raster scanning order.

To summarize the proposed orientation adaptive interpolation scheme, we first pick out the set of M_n, N_n according to the definition and formulate data matrix C and data vector $\vec{y}$. Then we use (5) to derive the interpolation coefficients $\vec{a}$. Finally, we substitute the derived coefficients into (2) and obtain the interpolation result. It should be noted that since some neighbors of X_n might not be available, we have to check the validity of the elements in both N_n and M_n. Throughout this paper, we define the set N_n to be the eight nearest neighbors of X_n and the set M_n to be the $(2T+1)^2-1$ neighbors of X_n within a square window sized by $(2T+1)\times(2T+1)$ and centered at X_n (refer to Fig. 2). An element in the set N_n is said to be *valid* if it is either successfully received or previously recovered. All the valid elements of N_n form the *valid set* N_n^*. Accordingly, an element in the set M_n is *valid* if the elements contained in its valid set N_n^* are all valid; and all the valid elements in the set M_n form the *valid set* M_n^*. So we always only use the valid set N_n^* and M_n^* during the interpolation.

IV. Linear Merge Strategy

Within the framework of sequential recovery, we still have another dimension of freedom, i.e., the choice of scanning order. First, according to our definition at the end of last section, different scanning orders render different valid set M_n^*, N_n^*, and thus affect the accuracy of recovering X_n. Second, since the previously recovered pixels $X_1, \ldots, X_{n-1}$ are being used to recover X_n, error propagation is inevitable and different scanning orders would result in different error-propagation patterns. Theoretically, there are K different orders when recovering K pixels. The computational complexity of exhaustively searching all scanning orders and taking the optimal one is prohibitive. In practice, the raster scanning order is often widely used due to its simplicity of implementation. Therefore, we focus on the limitations and remedies for raster scanning order in this section.

When the missing block is recovered in a raster scanning order, the valid set N_n^* typically contains the four nearest causal neighbors (refer to Fig. 3) and the valid set M_n^* has $2T(T+1)$ causal neighbors. The only exception is the pixels on the border of the corrupted block. For example, the valid set N_n^* of the pixel at the bottom-right corner is identical to N_n and its valid set M_n^* could include noncausal neighbors as well. It is easy to observe that the raster scanning makes a biased use of the local information during the recovery. The neighbors in the top-left half plane are more often used than the ones in the bottom-right half plane. Consequently, the recovery accuracy is not uniform inside the block. The pixels in the top-left quarter plane are usually more accurately recovered than those in the bottom-right quarter plane.

(a) (b)

Fig. 4. (a) Reconstructed Lena image in the raster scanning order for 25% isolated block loss (PSNR $= 25.26$ dB). (b) Error magnitude inside the 8×8 block.

Fig. 4 shows the Lena image recovered in the raster scanning order for nearly 25% isolated block loss (block size is 8 $\times$ 8). The peak signal-to-noise ratio (PSNR) value shown in the figure is computed using (8), as defined in Section V. It can be observed that, due to the orientation adaptive property of our interpolation, most edges are reasonably well recovered. However, noticeable artifacts can be found around some areas (e.g., the upper lip) due to error propagation. We can also see that the distribution of error magnitude is not uniform. The error pattern shown in Fig. 4 is associated with a specifically chosen orientation of the raster scanning, i.e., from left to right and from top to bottom.

A natural way to overcome the above error-propagation problem is to change the orientation of scanning order. It is easy to see that there are eight different orientations in total, as shown in Fig. 5. Each of them is associated with a specific error-propagation pattern. Therefore, we propose to take the linear merge of the eight versions recovered from different scanning orientations as the final result

$$X_n = \sum_{k=1}^{8} \omega_n^k X_n^k, \qquad (n = 1, \ldots, B \times B) \tag{6}$$

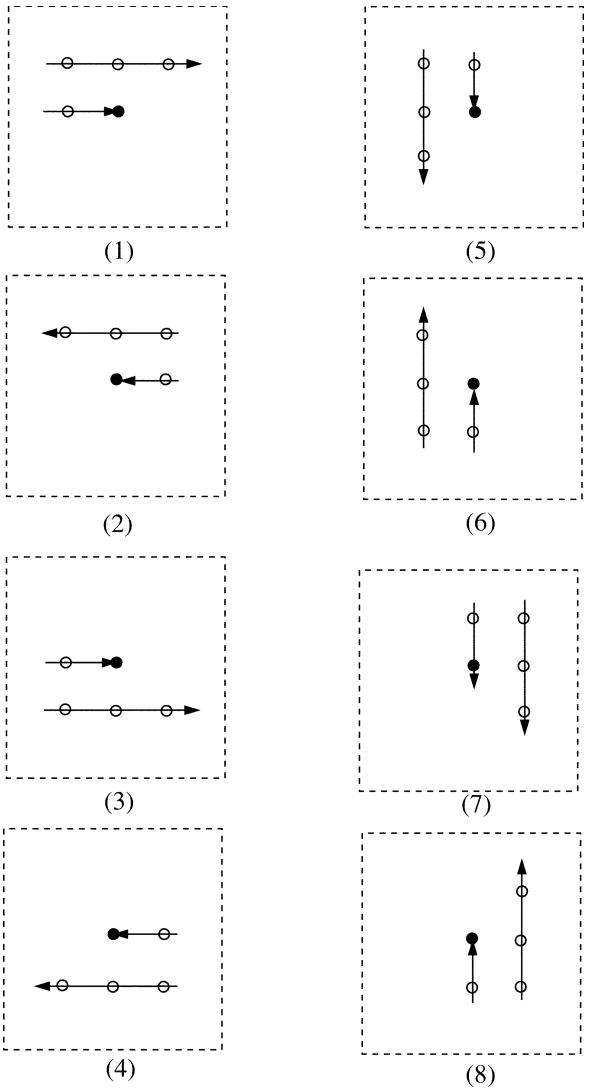

Fig. 5. Eight different scanning orders.

where X_n^k is the recovered X_n in the kth version and ω_n^k is the weighting coefficients controlling the contribution of the kth version at the location of X_n. We note that a convenient way to obtain all eight different scanning orders in the implementation is to flip the image by the combination of the following three patterns: left-to-right,up-to-down, and along the diagonal.

Intuitively, the linear merge strategy attempts to alleviate the error-propagation problem by intelligently weighting the results obtained from different orientations. The eight weighting coefficients ω_n^k ($k = 1$–8) clearly play the important role in the overall recovery performance. Though it is possible to optimize the weight assignment through an off-line training process, we find that the optimized weights through off-line training are often tuned to match the statistics of training images only and lose the generality. Therefore, we prefer to design a set of image-independent weights. Our weight design is based on the following two intuitive observations: 1) the spatial correlation decreases as the distance between two pixels increases and 2) the assigned weights should reflect the reliability of a specific scanning orientation at different spatial locations. For example, for the pixel at the top-left corner, ω^1 and ω^5 should be assigned more weight than ω^4 and ω^8 because the reconstructed value from the first and the fifth scanning orientations (left-to-right, top-to-bottom) are more trustworthy than those obtained from the fourth and the eighth (right-to-left, bottom-to-top).

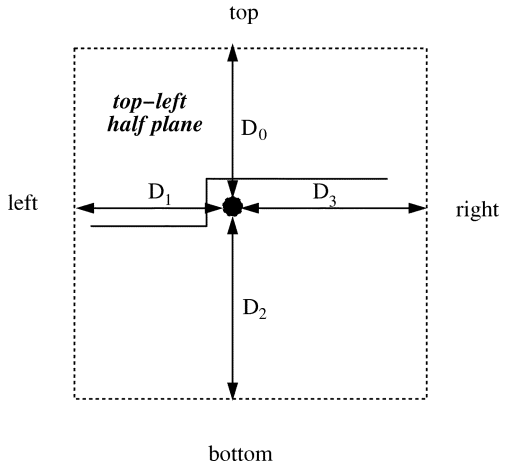

Fig. 6. Definition of distances D_k ($k = 0, 1, 2, 3$).

TABLE I
PAIR OF (a, b) IN DIFFERENT SCANNING ORIENTATIONS

k	1	2	3	4	5	6	7	8
a	0	0	2	2	1	1	3	3
b	1	3	1	3	0	2	0	2

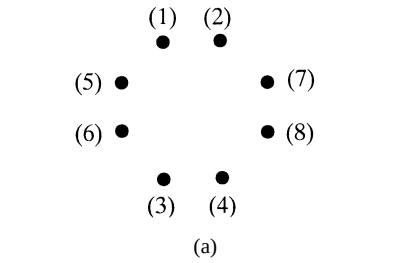

(a)

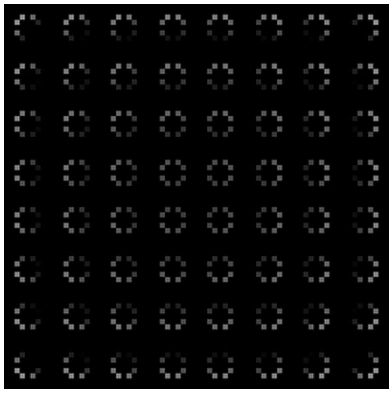

(b)

Fig. 7. (a) Constellation definition. (b) Weight distribution inside the block.

To implement the above ideas, we first compute the distances of any given pixel X_n to the four borders of the block: D_k ($k = 0, 1, 2, 3$) (refer to Fig. 6). Then we propose to calculate the eight weighting coefficients by

$$\omega_n^k = 0.25 - \frac{3D_a + D_b}{8S} \tag{7}$$

(a) (b) (c)

Fig. 8. (a) Corrupted image with 25% isolated block loss. (b) Corrupted image with 50% consecutive block loss. (c) Corrupted image with both isolated and consecutive block loss.

where $S = \sum_{k=0}^{3} D_k$ and pair (a, b) is given by Table I. It can be justified that the larger distance D_k is, the smaller weight is assigned, which matches our first assumption. Meanwhile, the choice of the pair (a, b) is designed to intuitively reflect the reliability of different scanning orientations. Finally, we note that $\sum_{k=1}^{8} \omega_n^k$ is always equal to 1.

Fig. 7 graphically shows the assigned weighting coefficients inside a 8×8 block given by (7). There are 8×8 constellations, each corresponding to one pixel inside the 8×8 block. Each constellation is composed of eight dots whose gray value is proportional to the magnitude of eight coefficients ω_n^k $(k = 1, \ldots, 8)$. It can be seen that, for the pixel at the top-left corner, ω^1 and ω^5 are indeed assigned much more weight than ω^4 and ω^8. As we shall see from the experiment results next, the linear merge strategy substantially enhances the performance of sequential recovery though at the price of increased computational complexity by a factor of eight.

Finally, we want to note that the proposed linear merge strategy can be viewed as a low-complexity approximation of a globally optimized solution to the problem of maximizing (1). In fact, one of well-known stochastic optimization techniques for solving the problem of maximizing the conditional probability of each individual pixel given the observations and the other pixel estimates is the ICM method [17]. Since the ICM method also employs Bayes' rule, it suffers from a similar limitation as [15]. However, the idea of iteratively recovering the image can also be applied to our sequential approach. The above-described error-concealment technique can be viewed as "the first iteration." Since the first iteration already resolves much uncertainty about the missing pixels, it is natural to take it as the basis for refining the recovery result. Intuitively, the least-square estimation should achieve more accurate results because the valid set M_n^* contains more relevant information about X_n after the first iteration and recursively applying the proposed technique might converge after finite iterations. However, we do not recommend such iterative technique in practice due to its prohibitive computational complexity.

V. Simulation Results

To compare our sequential error-concealment techniques with previous parallel techniques, we use the traditional PSNR as the objective measure in our experiments. PSNR is defined by

$$\mathrm{PSNR} = 10 \log_{10} \frac{255^2}{\mathrm{MSE}} \tag{8}$$

where MSE is the normalized mean-square difference between the original blocks and the reconstructed blocks

$$MSE = \frac{1}{|N_{\mathrm{cb}}|} \sum_{b \in N_{\mathrm{cb}}} \left\{ \frac{1}{B^2} \sum_{i=1}^{B} \sum_{j=1}^{B} (X_{i,j}^b - \dot{X}_{i,j}^b)^2 \right\} \tag{9}$$

where N_{cb} is the collection of all corrupted blocks and $\dot{X}$ is the reconstructed image. It should be noted that the PSNR value given by (8) and (9) is usually smaller than the PSNR value computed for the entire image that is commonly used in image coding. The difference between the two PSNR values is a constant which is dependent on the block-loss ratio θ.

1. 8 × 8 Block

Previous works [13], [14] have considered the situation of the 8×8 block. Three different block-loss situations are investigated (as shown in Fig. 8):

1) isolated block loss ($\theta \approx 25\%$);
2) consecutive block loss ($\theta \approx 50\%$);
3) mixture of isolated and consecutive block loss ($\theta \approx 10\%$).

Table II includes the PSNR comparison results between [13], [14], and ours for the Lena image in various block-loss situations. The PSNR performance improvement over [14] ranges from 0.6 to 0.8 dB. It appears that the improvement on the visual quality is more impressive than the PSNR values. Fig. 9 shows the comparison of the reconstructed Lena images given by [13], [14], and our new technique in the situation of 25% isolated block loss. It can be observed that the new technique has achieved noticeable improvements in the area of complex texture structures. Local structures such as streaks and corners are recovered with better fidelity. For better subjective evaluation, the enlarged portions around the hairs are shown in Fig. 10. Several portions where new technique outperforms previous ones are highlighted in the original image.

Fig. 9. (a) Original Lena image. (b) Reconstructed image by [13], PSNR $= 26.34$ dB. (c) Reconstructed image by [14], PSNR $= 27.43$ dB. (d) Reconstructed image by our scheme, PSNR $= 28.25$ dB.

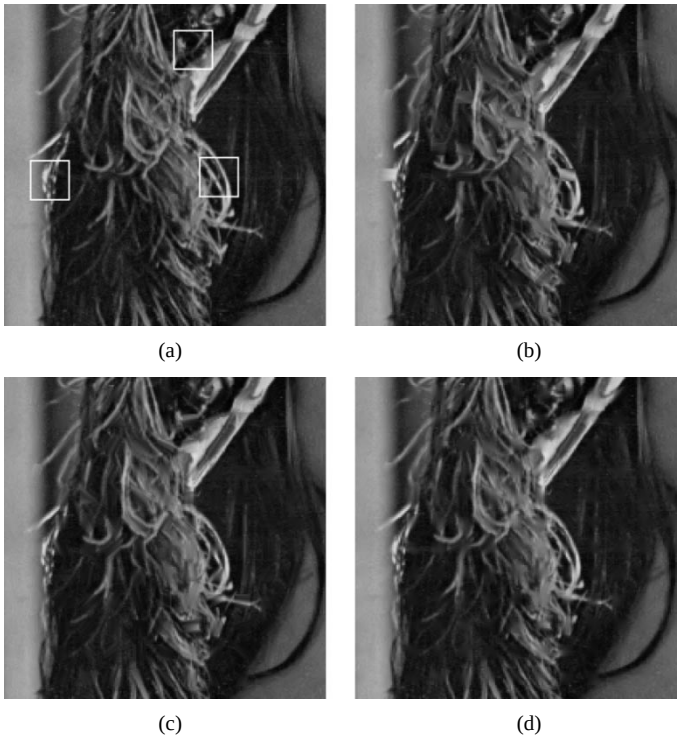

Fig. 10. Comparison of the zoomed portions in Fig. 9.

2. 16 × 16 Block

Most previous works on error concealment [3]–[7] have studied the case of 16 × 16 block. Two different block-loss situations are popularly considered (refer to Fig. 11):

1) isolated block loss ($\theta \approx 10\%$);
2) consecutive block loss ($\theta \approx 25\%$).

TABLE II
PERFORMANCE COMPARISON IN PSNR (DECIBELS) FOR LENA IMAGE

Block loss case	Jung's [13]	Zeng's [14]	Ours
25% isolated block loss	26.34	27.43	28.25
50% consecutive block loss	-	27.28	27.88
10% mixed block loss	-	26.60	27.38

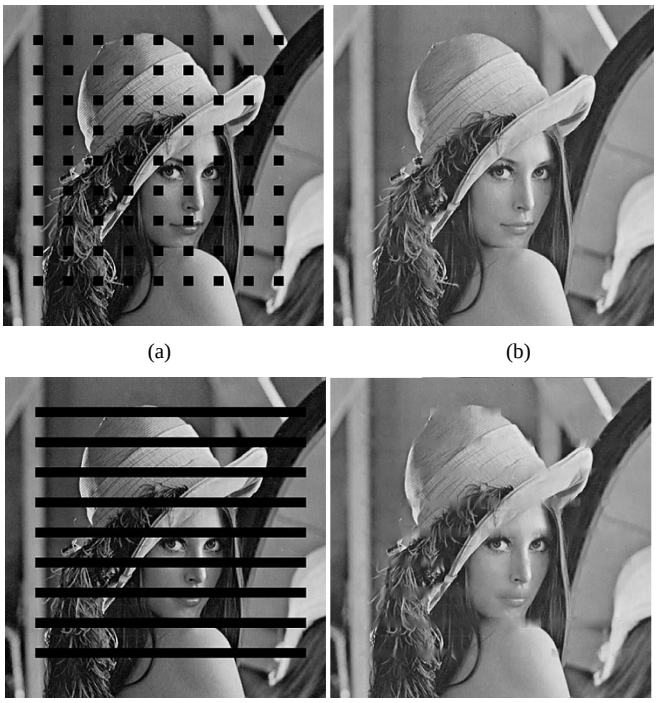

Fig. 11. (a) Corrupted Lena image (isolated block loss). (b) Reconstructed image by our scheme (PSNR $= 26.46$ dB). (c) Corrupted Lena image (consecutive block loss). (d) Reconstructed image by our scheme (PSNR $= 23.55$ dB).

TABLE III
PERFORMANCE COMPARISON IN PSNR (DECIBELS) FOR ISOLATED BLOCK LOSS

Image	Salama's	Wang's	Sun's	Park's	Ours
Lena	23.99	24.41	23.93	24.96	26.46
Pepper	23.69	24.06	22.19	24.48	27.25
Zelda	27.13	26.40	26.35	27.36	28.33

TABLE IV
PERFORMANCE COMPARISON IN PSNR (DECIBELS) FOR CONSECUTIVE BLOCK LOSS

Image	Salama's	Wang's	Sun's	Park's	Ours
Lena	19.90	20.92	20.14	22.42	23.55
Pepper	20.34	20.87	19.12	21.33	25.23
Zelda	22.39	23.37	22.17	23.68	26.14

We cite the PSNR results of [3]–[5], [7] from [7] during the comparison. It can be seen from Tables III and IV that we have achieved 1.0–2.8 dB improvement in the case of isolated block loss and 1.1–3.9 dB improvement in the case of consecutive block loss over the best published results in the literature. Fig. 11 shows the corrupted Lena images and the reconstructed images given by our new technique in both block-loss situations. Noticeable improvements can be found around the edges (e.g., the

hairs and the rim of the hat) by comparing our results with the results shown in [7].

VI. Concluding Remarks

In this paper, we present a novel sequential framework for error concealment. Within the framework of sequential recovery, it becomes possible to model the dependency within the image on a pixel-by-pixel basis instead of on a block-by-block basis. The sequential recovery framework provides a better ground for improving the capability of handling complex image structures and serious block-loss situations. We present a novel orientation-adaptive interpolation scheme and investigate the problem with error propagation. To fight against error propagation, we propose to recover the missing block from eight different scanning orientations and take their linear merge as the final result. Our experiment results have justified the superiority of sequential error-concealment techniques. Impressive improvements on both objective and subjective measure have been achieved.

References

[1] W. Pennebaker and J. Mitchell, *JPEG Still Image Data Compression Standard*. Norwell, MA: Kluwer, 1992.

[2] J. Mitchell, W. Pennebaker, and C. E. Fogg, *MPEG Video: Compression Standard*. Norwell, MA: Kluwer, 1996.

[3] Y. Wang and Q. Zhu, "Signal loss recovery in DCT-based image and video codecs," in *Proc. SPIE Conf. Visual Communication and mage Processing*, vol. 1605, Nov. 1991, pp. 667–678.

[4] H. Sun and W. Kwok, "Concealment of damaged block transform coded images using projection onto convex set," *IEEE Trans. Image Processing*, vol. 4, pp. 470–477, Apr. 1995.

[5] P. Salama, N. B. Shroff, E. J. Coyle, and E. J. Delp, "Error concealment techniques for encoded video streams," in *Proc. Int. Conf. Image Processing*, vol. I, Oct. 1995, pp. 9–12.

[6] J. W. Park, J. W. Kim, and S. U. Lee, "DCT coefficients recovery-based error concealment technique and its application to the MPEG-2 bit stream error," *IEEE Trans. Circuits Syst. Video Technol.*, vol. 7, pp. 845–854, Dec. 1997.

[7] J. W. Park and S. U. Lee, "Recovery of corrupted image data based on the NURBS interpolation," *IEEE Trans. Circuits Syst. Video Technol.*, vol. 9, pp. 1003–1008, Oct. 1999.

[8] X. Lee, Y. Zhang, and A. Leon-Garcia, "Information loss recovery for block-based image coding techniques—A fuzzy logic approach," *IEEE Trans. Image Processing*, vol. 4, pp. 259–273, Mar. 1995.

[9] J.-W. Suh and Y.-S. Ho, "Error concealment based on directional interpolation," *IEEE Trans. Consumer Electron.*, vol. 43, pp. 295–302, Aug. 1997.

[10] Z. Wang, Y. Yu, and D. Zhang, "Best neighborhood matching: An information loss restoration technique for block-based image coding systems," *IEEE Trans. Image Processing*, vol. 7, pp. 1056–1061, Jul. 1998.

[11] W.-M. Lam and A. Reibman, "An error concealment algorithm for images subject to channel errors," *IEEE Trans. Image Processing*, vol. 4, pp. 533–542, May 1995.

[12] W. Zhu, Y. Wang, and Q. Zhu, "Second-order derivative-based smoothness measure for error concealment in DCT-based codecs," *IEEE Trans. Circuits Syst. Video Technol.*, vol. 8, pp. 713–718, Oct. 1998.

[13] K. Jung, J. Chang, and C. Lee, "Error concealment technique using projection data for block-based image coding," in *Proc. SPIE Conf. Visual Communication and Image Processing*, vol. 2308, 1994, pp. 1466–1476.

[14] W. Zeng and B. Liu, "Geometric-structure-based directional filtering for error concealment in image/video transmission," in *Proc. SPIE Conf. Wireless Data Transmission, Photonics East*, vol. 2601, Oct. 1995, pp. 145–156.

[15] P. Salama *et al.*, "Error concealment in MPEG video streams over ATM networks," *IEEE Trans. Select. Areas Commun.*, vol. 18, pp. 1128–1144, Jun. 2000.

[16] X. Li and M. Orchard, "Edge directed prediction for lossless compression of natural images," *IEEE Trans. Image Processing*, vol. 10, pp. 813–817, Jun. 2001.

[17] J. Besag, "On the statistical analysis of dirty pictures," *J. Roy. Statist. Soc. B*, vol. 48, no. 3, pp. 259–302, 1986.

[18] Y. Wang and Q. Zhu, "Error control and concealment for video communication: A review," *Proc. IEEE*, vol. 86, pp. 974–997, May 1998.

[19] M. Robertson and R. Stevenson, "DCT quantization noise in compressed images," in *Proc. Int. Conf. Image Processing*, vol. 1, Oct. 2001, pp. 185–188.

[20] N. Jayant and P. Noll, *Digital Coding of Waveforms: Principles and Applications to Speech and Video*. Englewood Cliffs, NJ: Prentice-Hall, 1984.

[21] A. Papoulis, *Probability, Random Variables and Stochastic Process*. New York: McGraw-Hill, 1984.

Xin Li (S'97–M'00) received the B.S. degree (with highest honors) in electronic engineering and information science from University of Science and Technology of China, Hefei, in 1996, and the Ph.D. degree in electrical engineering from Princeton University, Princeton, NJ, in 2000.

He has been a Member of Technical Staff with Sharp Laboratories of America, Camas, WA, since August 2000. His research interests include image/video coding and processing.

Dr. Li received the Best Student Paper Award at the Conference of Visual Communications and Image Processing, San Jose, CA, in January 2001.

Michael T. Orchard (F'00) was born in Shanghai, China. He received the B.S. and M.S. degrees in electrical engineering from San Diego State University, San Diego, CA, in 1980 and 1986, respectively, and the M.A. and Ph.D. degrees in electrical engineering from Princeton University, Princeton, NJ, in 1988 and 1990 respectively.

He was with the Government Products Division, Scientific Atlanta, from 1982 to 1986, developing passive sonar DSP applications, and has consulted with the Visual Communication Department of AT&T Bell Laboratories since 1988. From 1990 to 1995, he was an Assistant Professor with the Department of Electrical and Computer Engineering, University of Illinois at Urbana-Champaign, where he served as Associate Director of Image Laboratory, Beckman Institute. From 1995 to 2000, he was an Associate Professor with the Department of Electrical Engineering, Princeton University. Since the spring of 2000, he has been with the Department of Electrical and Computer Engineering at Rice University, Houston, TX.

Dr. Orchard received the National Science Foundation Young Investigator Award in 1993, the Army Research Office Young Investigator Award in 1996, and was elected IEEE Fellow in 2000 for "contribution to the theory and development of image and video compression algorithms".